REGIONAL MODELING OF GREENLAND'S OUTLET GLACIERS WITH THE PARALLEL ICE SHEET MODEL

By

Daniella N. Della-Giustina

RECOMMENDED:

Advisory Committee Chair

Chair, Department of Physics

APPROVED:

Dean, College of Natural Science and Mathematics

Dean of the Graduate School

Dec 6, 2011

Date

REGIONAL MODELING OF GREENLAND'S OUTLET GLACIERS WITH THE PARALLEL ICE SHEET MODEL

A

THESIS

Presented to the Faculty

of the University of Alaska Fairbanks

in Partial Fulfillment of the Requirements

for the Degree of

MASTER OF SCIENCE

By

Daniella N. Della-Giustina, B.S.

Fairbanks, Alaska

December 2011

Abstract

The most recent report from the Intergovernmental Panel on Climate Change cites ice sheet dynamics as the greatest source of uncertainty for predicting current and future rates of sea level rise. This has prompted the development and use of ice sheet models that are capable of simulating the flow and evolution of ice sheets and their corresponding sea level contribution. In the Arctic, the Greenland ice sheet appears to be responding to a warming climate more quickly than expected. In order to determine sea level contribution from Greenland, it is necessary to capture the regional dynamics of the fast flowing outlet glaciers that drain the ice sheet.

This work has developed a novel regional model capable of simulating an outlet glacier, and its associated drainage basin, as a mode of using the Parallel Ice Sheet Model. Specifically, it focuses on modeling the Jakobshavn Isbræ as a demonstration. The Jakobshavn Isbræ is one of the world's fastest flowing outlet glaciers, and accounts for nearly 5% of ice loss from the Greenland Ice Sheet. Additionally, the Jakobshavn Isbræ has been widely studied for several decades, and a wealth of remotely sensed and in situ data is available in this region. These data are used as model input and for model validation.

We have completed a parameter study in this work to examine the behavior of the regional model. The purpose of this study was not to tune the model to match observations, but rather to look at the influence of parameter choices on the ice dynamics. Model results indicate that we have identified the subset of the model parameter space that is appropriate for modeling this outlet glacier. Additionally, we are able to produce some of this more interesting features that have been observed at Jakobshavn, such as the development and disintegration of a floating ice tongue and the distribution of observed surface velocities. We validate these model results by comparison with recent spatially rich measurements of ice surface speeds, as well as ice geometry.

Table of Contents

Signature Page i
Title Page ii
Abstract iii
Table of Contents iv
List of Figures vi
List of Tables viii
Acknowledgements ix
Chapter 1 Introduction 1
1.1 Background 1
1.2 Thesis Overview 3
Chapter 2 Methods 4
2.1 The Parallel Ice Sheet Model 4
2.2 Tools for Regional Modeling 4
2.2.1 Drainage Basin Identification 5
2.2.2 Boundary Conditions 11
2.2.3 Force-to-thickness Mechanism 12
2.3 Modeling Choices 13
2.3.1 Basal resistance 13
2.3.2 Calving Style 14
2.3.2.1 Calving Floating Ice 15
2.3.2.2 Calving Ice at Present-day Calving Front 15
2.3.2.3 Eigen-Calving at Thickness 15
2.3.3 Sub-shelf Ocean Heat Flux 16
Chapter 3 Results 17
3.1 The Jakobshavn Regional Ice Sheet Model 17
3.1.1 Modeling Input 17
3.2 Experiments 18
3.3 Model Validation 19
Chapter 4 Discussion and Conclusions 29
4.1 Performance 29

4.2 Capability of the PISM Regional Model 30
4.3 Future Work 32
Chapter 5 Conclusions 35
Bibliography 36

List of Figures

2.1 The process of defining a DB and the regional model domain: (a) Ice surface elevation provided by [1]. (b) Streamlines that follow the ice surface elevation as determined by the DB generator algorithm. (c) The pink user-defined TERM box that indicates the approximate location of the glacier terminus. The origin of streamlines that end in the TERM after N perturbations are considered part of the DB. (d) The blue rectangle defines the boundaries of the regional model domain, which contains the DB. 7

2.2 The domain of a regional model in PISM. 8

2.3 The area of a drainage basin as a function of two user specified parameters: (dark blue) the number of perturbations N and (light green) the standard deviation d of the mean distribution used to generate the perturbations (in km). 9

2.4 The average area of a drainage basin, for ten different runs of the generator, with respect to grid cell size. Here the error bars indicate the range of drainage basin areas determined by the generator, for $d = 5$ km and $N = 3$. Consecutive runs of the drainage basin generator with the same parameter values yield slightly different results because of the random element introduced by perturbing streamline origins. Although we only examined the dependence of basin area on grid cell size for 1 km and 5 km grids, ideally this plot will converge to the "true" area of the drainage basin as grid cell size approaches zero. 10

3.1 A flowchart that depicts the procedure used to generate and validate all of the model results in this parameter study. 25

3.2 Distribution of modeled and observed surface speeds for 2 km experiments. 26

3.3 Distribution of modeled and observed surface speeds for 1 km experiments. 27

3.4 Map-plane view of modeled and observed surface speeds for 1 km experiments. (From top to bottom) Observed, Eigen-calving, Float-kill, and Ocean-kill surface speeds. 28

4.1 Snapshots of the the age-tracer experiment at (a) 0 model years, (b) 500 model years, and (c) 1000 model years. Here red indicates the position of the coastline, blue and green represent the surface speeds and basal speeds, respectively (m a $^{-1}$), and black indicates areas of old ice. Courtesy of Constantine Khroulev. 34

List of Tables

3.1 Regional model components and inputs. 18
3.2 Velocity comparison for 2 km calving-style study. 22
3.3 Geometry comparison for 2 km calving-style study. 22
3.4 Velocity comparison for 2 km ocean heat flux study. 23
3.5 Geometry comparison for 2 km ocean heat flux study. 23
3.6 Velocity comparison for 1 km parameter study. 24
3.7 Geometry comparison for 1 km parameter study. 24

Acknowledgements

First and foremost I would like to thank Andy Aschwanden and Constantine Khroulev. Much of the work presented in this Thesis is the result of their guidance, technical support, and (endless) patience.

This work would not have been possible without the expertise of my advisors Ed Bueler and Martin Truffer. They helped me define the scope of this project, and presented me with thought provoking challenges in both coursework and research. Moreover, I would like to thank them for their understanding and flexibility, which allowed me change my program of study, complete part of my work remotely, and also attend a field campaign in Greenland during the spring of 2010. I would like to thank Renate Wackerbauer, the third member of my committee, for introducing me to the study of complex dynamic systems, and also for adding her "outsiders" perspective to this work.

I would like to thank Chris Larsen, who showed me around the Geophysical Institute during the summer of 2008, when I was a prospective UAF graduate student. Regine Hock was also very helpful during my initial months in Fairbanks, AK and provided me with my first exposure to the academic study of glaciers.

And, of course, I'd like to thank my family for their encouragement and perpetual support of my academic endeavors.

This work was funded by NASA's Modeling, Analysis, and Prediction program (grant #NNX09AJ38G) and was also supplemented by a 2010-2011 Student Research Grant from the Center for Global Change. Supercomputing time and technical support was provided by the Arctic Region Supercomputer Center.

Chapter 1
Introduction

1.1 Background

The present day polar ice sheets include Greenland and Antarctica, and store more than 99% of the fresh water on Earth. Understanding the evolution of ice sheets in response to climate change is of scientific and societal importance; the polar ice sheets contain enough fresh water to raise the global sea level by 64 m if fully melted [1], [2].

At present, Greenland and Antarctica account for 30% and 10% of the eustatic contribution to sea level rise, respectively [3]. Both ice sheets are reacting to climate change more immediately than expected. The Antarctic ice sheet is rapidly losing mass due to accelerating ice flow in coastal regions [4], as is the Greenland ice sheet [5]. Currently, the observed rate of sea level rise is at, or extends above, the upper limit of predicted rates [6]. This range of estimated rates has been determined by global circulation models (GCMs), which only consider the effect of changing surface mass balance on ice sheets. Although these are important components, the sea level contribution due to ice flow (dynamics) is entirely neglected. The latest report from the Intergovernmental Panel on Climate Change (IPCC) cites ice sheet and glacier dynamics as the largest source of uncertainty for predicting sea level rise [7]. Ice sheet models capable of simulating the evolution of ice dynamics are needed, as well as GCMs capable of coupling to such models.

Continental ice sheets maintain large interior reservoirs of slow-moving ice, which are drained at coastal margins by fast flowing outlet glaciers (rapid ice flow through deep bedrock channels) and/or ice streams (rapid ice flow through wide and shallow channels overlaying a weak base). Combined, these fast flowing features account for 90% of the ice discharge rate from the Antarctic ice sheet [8], and increasingly fast ice flow from outlet glaciers accounts for roughly 66% of total ice discharge from Greenland [9]. The largest uncertainty in constraining sea level contribution from Greenland, however, lies in the ability of a model to capture changes in the outlet systems [10]. Efforts are being made to understand the dynamics and long-term behavior of these regional features, and their influence on the entirety of the ice sheet. Observations of ice flow velocities in these regions are made by GPS measurements [11] and synthetic aperture radar [12]. Predicting the long-

term behavior, however, will require detailed regional ice sheet modeling.

Since the last IPCC Assessment Report (AR4), a number of ice sheet models are available to address the need for dynamic modeling of ice flow. However, these large, continental scale ice sheet models often fail to capture the fast flowing behavior of outlet glaciers and ice streams. Typically, dynamic ice sheet models are only capable of simulating the evolution of an ice sheet on a continental (not regional) scale and there remains little about regional ice sheet models in the scientific literature. Although some regional scale models of outlet glaciers have been developed [13], [14], [15], these are flow-line models and provide information about the dynamic state of an ice sheet region. Higher order regional models may also have to restrict their analysis to a flow-line because of the computational cost [15].

High resolution modeling ($\leq$ 1 km grid cell spacing) is necessary to capture the important features of an outlet glacier's dynamic evolution. The trunk of these glaciers is typically no wider then 5 km, and an outlet glacier model should also be capable of resolving the details of grounding line motion. Running a simulation of an entire ice sheet at high resolution requires significant computational resources, which are expensive and may not be readily available. Shared computing resources, such as supercomputers, may also limit the wall-clock time available for a given model run, therefore a tradeoff exists between grid resolution and the desired run length (in model years). Although some of these issues can be addressed by using adaptive grids or meshes in a model, these capabilities are not present in the Parallel Ice Sheet Model (PISM).

PISM is an open source ice sheet model developed at the University of Alaska, Fairbanks. The model originated from a numerical shallow ice approximation of the Antarctic ice sheet [16]. PISM performs finite difference calculations of two shallow ice approximations for the stress balance equations of nonlinear viscous flow [17], as well as an enthalpy-based conservation of energy scheme [18]. The goal of this project is to extend the capability of PISM by supporting regional modeling of Greenland's and Antarctica's outlet glaciers. Prior to this work, the PISM source code only supported continental scale modeling.

In particular, this work used the Jakobshavn Isbræ as an example to demonstrate PISM's ability to perform regional ice sheet modeling. The Jakobshavn Isbræ is one of the most

dynamic outlet glaciers in Greenland and its behavior has been extensively studied for nearly three decades [19], [20], [21]. The wealth of remotely-sensed and in situ data available at Jakobshavn makes it the ideal test case for a regional ice sheet model. These data are used both as model input and for model validation.

1.2 Thesis Overview

This work has developed a scheme capable of modeling a single outlet glacier of the Greenland ice sheet using and modifying PISM. Specifically, it focuses on modeling the Jakobshavn Isbræ as a demonstration. The model results are validated by comparison to spatially rich synthetic aperture radar observations of ice surface speed [22] and a digital elevation model [1], [23].

Chapter 2 describes the computational methods developed to overcome challenges associated with regional modeling. Chapter 3 provides an overview of the parameter study and numerical experiments for a model test case of the Jakobshavn Isbræ. Chapter 4 discusses and interprets the model results, and investigates improvements that could be made in future regional models. Chapter 5 concludes with a summary and final thoughts.

Chapter 2
Methods

2.1 The Parallel Ice Sheet Model

PISM was developed to perform continental scale ice sheet modeling of present-day and paleo-ice sheets. In particular, the aim of whole Greenland PISM simulations is to produce a dynamical system which evolves over time as similarly as possible to the entire Greenland ice sheet. PISM is a sophisticated C++ ice sheet modeling code that uses the Portable Extensible Toolkit for Scientific computing (PETSc) and a Message Passing Interface (MPI). This allows PISM to run high-resolution simulations in parallel on large supercomputers. PISM currently solves the shallow ice approximation (SIA) and shallow shelf approximation (SSA) for nonlinear ice flow, in the ice-covered portion of the rectangular computational domain [17]. The SIA describes ice as flowing by shear in planes parallel to the geoid, with a strong contact of ice base to bedrock, while the SSA describes a membrane-type flow of floating ice or of grounded ice that is sliding over a weak base. The evolution of both temperature and water fraction in the ice is captured by the energy state using a polythermal enthalpy-based scheme [18].

Ice sheet initial conditions, which are not typically observable in an ice sheet, are obtained during a stage referred to as "bootstrapping". During bootstrapping, a model run is initiated using observable quantities such as ice thickness and surface temperature while heuristics are used in order to fill in temperatures at depth, and estimate basal sliding conditions. After bootstrapping, a long "spin-up" run (typically tens of thousands of years) is performed to allow the ice to evolve toward a more physical steady state, which will have a compatible temperature field, age field, and velocities. This procedure allows one to obtain the initial conditions in the ice that are used for a simulation. During bootstrapping, spin up, and the model run, surface boundary models for atmosphere, surface mass balance, and the ocean are applied; these models are discussed further in Chapter 3.

2.2 Tools for Regional Modeling

The most significant advantage of modeling on a regional (opposed to continental) scale, is the improvement that can be achieved in resolution. Modeling an entire ice sheet has resolution limitations (e.g. 5 km grid cells), while considering only the area of the specific

catchment can allow much higher resolution modeling (e.g. potentially 500 m grid cells). We have extended the capability of PISM by adding tools to perform regional-scale modeling of individual outlet glaciers. These tools can be automatically applied basin-by-basin to each outlet system on an ice sheet.

2.2.1 Drainage Basin Identification

When modeling an entire ice sheet the domain boundaries of the model are well defined; they are set well outside of the ice sheet margins (i.e. far from the coastline). When modeling only a region of the ice sheet, however, defining the domain boundary is less straightforward. To determine the model domain for an outlet glacier, it is important to include the entire glacier catchment while still minimizing the domain area. This ensures that the highest allowable resolution can be achieved during a model run.

To identify an outlet glacier drainage basin (DB) and the corresponding regional domain, we have developed a "drainage basin generator" algorithm. The algorithm the uses the assumption that ice flows down the surface gradient to determine the extent of a drainage basin. This idea has been applied in an ad hoc, by-hand manner for ice flow problems [24]. Although surface velocity data are available for much of Greenland, we choose to identify glacier catchments by calculating the surface gradient streamlines from a digital elevation model (DEM). Unlike surface velocity, the ice-sheet upper surface elevation is a contiguous dataset (Figure 2.1.a), which is available in high-accumulation areas and near slow-moving ice divides for both the ice sheets. Additionally, the extent of drainage-flow areas and the outer boundary of the basin are defined by slow moving ice, where measurements of surface velocity maintain substantial observational error [12]. Flow on the ice sheet that is not nearly down the surface gradient tends to be limited to areas of fast flow within (i.e. downstream in) a drainage basin, and not at the upstream boundaries.

In this work, we define streamlines as curves that are pointwise tangent to a surface gradient vector-field. These streamlines are assumed to indicate the horizontal path that a test particle will follow if the ice flows down the surface gradient. The "drainage basin generator" calculates surface gradient flow using centered finite difference approximations and determines the corresponding streamlines (Figure 2.1.b). These streamlines indicate where interior ice will exit the ice sheet. Ice that does not exit the ice sheet through the

user-specified terminus (TERM) area is excluded from the DB (Figure 2.1.c). Additionally, the generator randomly perturbs the origin of each streamline and then calculates down-gradient streamlines from perturbed points; if streamlines generated from the perturbed point also end in the TERM area, then we consider that original grid point is more likely to be part of the DB. This process of randomly perturbing grid points allows us to test the sensitivity of the DB margins that are defined by the generator. To ensure robustness and stability, only grid points that survive a number of user-specified perturbations, N, are kept as part of the DB area. The random perturbations (in km) are generated from a normal distribution, with a mean of zero and a user-specified standard deviation, d.

The procedure of calculating streamlines and perturbing their origins is repeated for each grid point that is potentially in the DB. After this procedure, the rectangular regional grid that encloses the basin is determined (Figure 2.1.d). We define the DB using an integer mask which allows us to divide the regional model into two distinct areas: a fully modeled outlet glacier catchment (DB area) and the surrounding ice that is modeled in a modified way (no model strip + force-to-thickness area). See Figure 2.2.

The drainage basin identification is performed by merely supplying a DEM and a user-specified rectangle (TERM area) for the approximate glacier terminus. From this information, the "drainage basin generator" determines the margins of the glacier catchment and these margins are used to define the minimum regional domain possible. The final result is a mask variable which delineates the drainage basin from surrounding ice, as well as the latitude-longitude bounds that define the domain area.

Comparison of several drainage basins created by the generator indicate that the basin area is not sensitive from run to run. We have confirmed this by varying user-specified inputs N and d, and examining how these parameters influence the area of the DB (Figure 2.3). Additionally, we have examined how the cell size of the grid used to determine the basin will affect the final DB area (Figure 2.4). Although the results of the DB generator display some dependence on N, d, and grid cell spacing, all DBs examined in this comparison are within 1% area of one another.

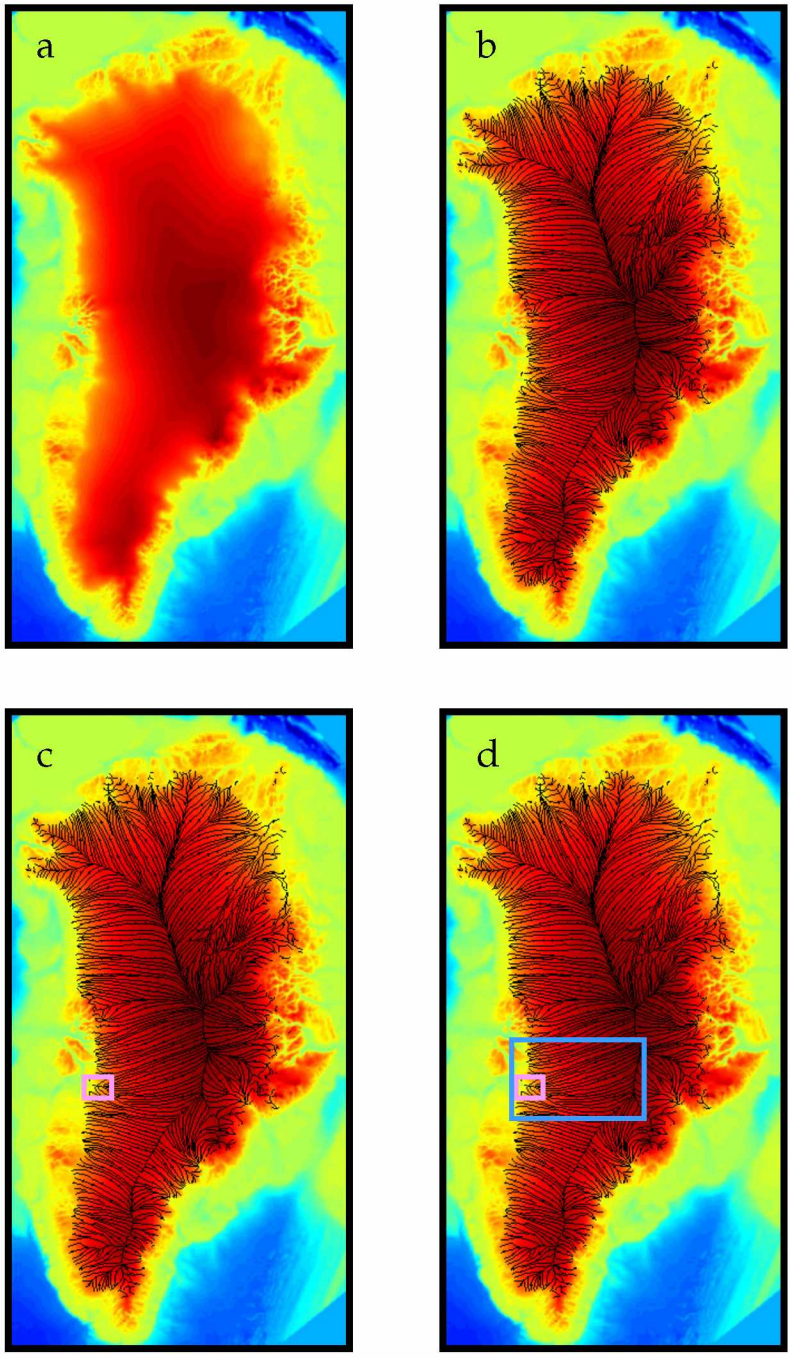

Figure 2.1. The process of defining a DB and the regional model domain: (a) Ice surface elevation provided by [1]. (b) Streamlines that follow the ice surface elevation as determined by the DB generator algorithm. (c) The pink user-defined TERM box that indicates the approximate location of the glacier terminus. The origin of streamlines that end in the TERM after N perturbations are considered part of the DB. (d) The blue rectangle defines the boundaries of the regional model domain, which contains the DB.

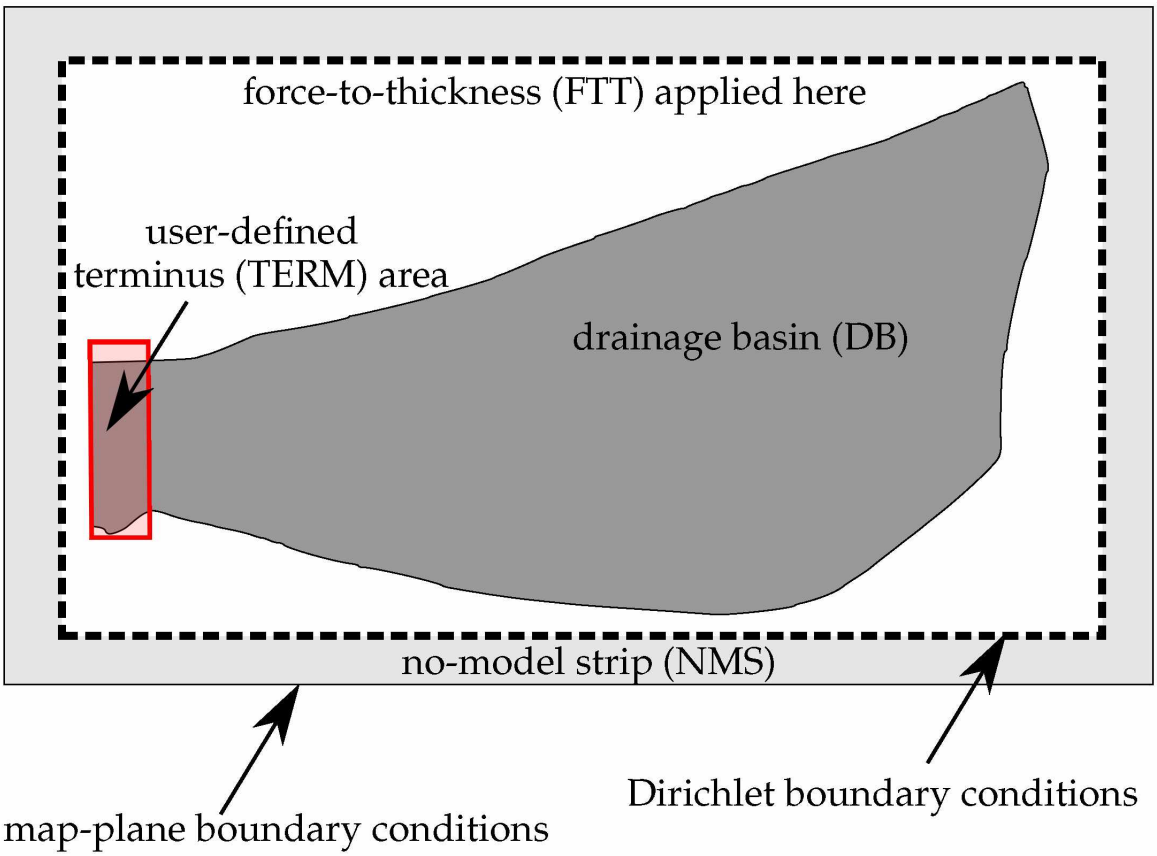

Figure 2.2. The domain of a regional model in PISM.

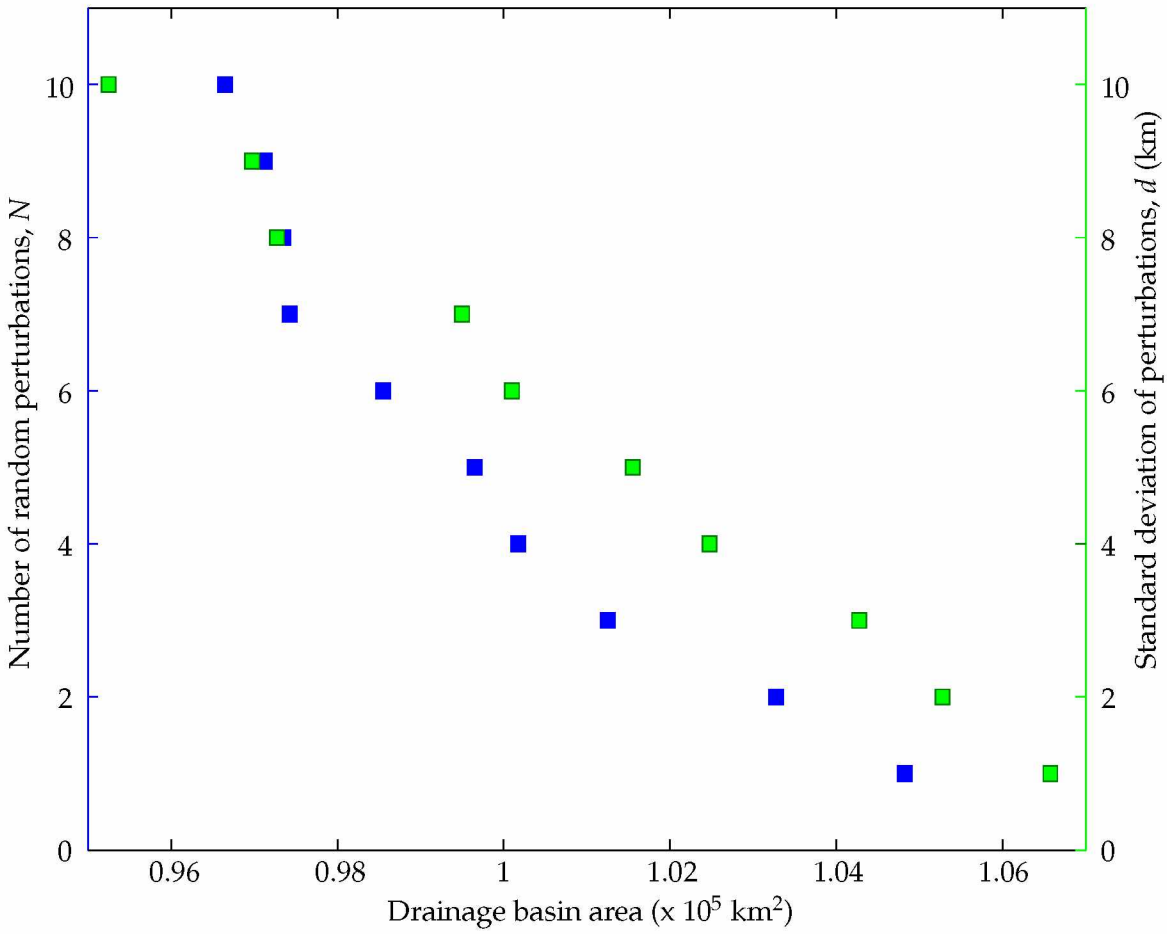

Figure 2.3. The area of a drainage basin as a function of two user specified parameters: (dark blue) the number of perturbations N and (light green) the standard deviation d of the mean distribution used to generate the perturbations (in km).

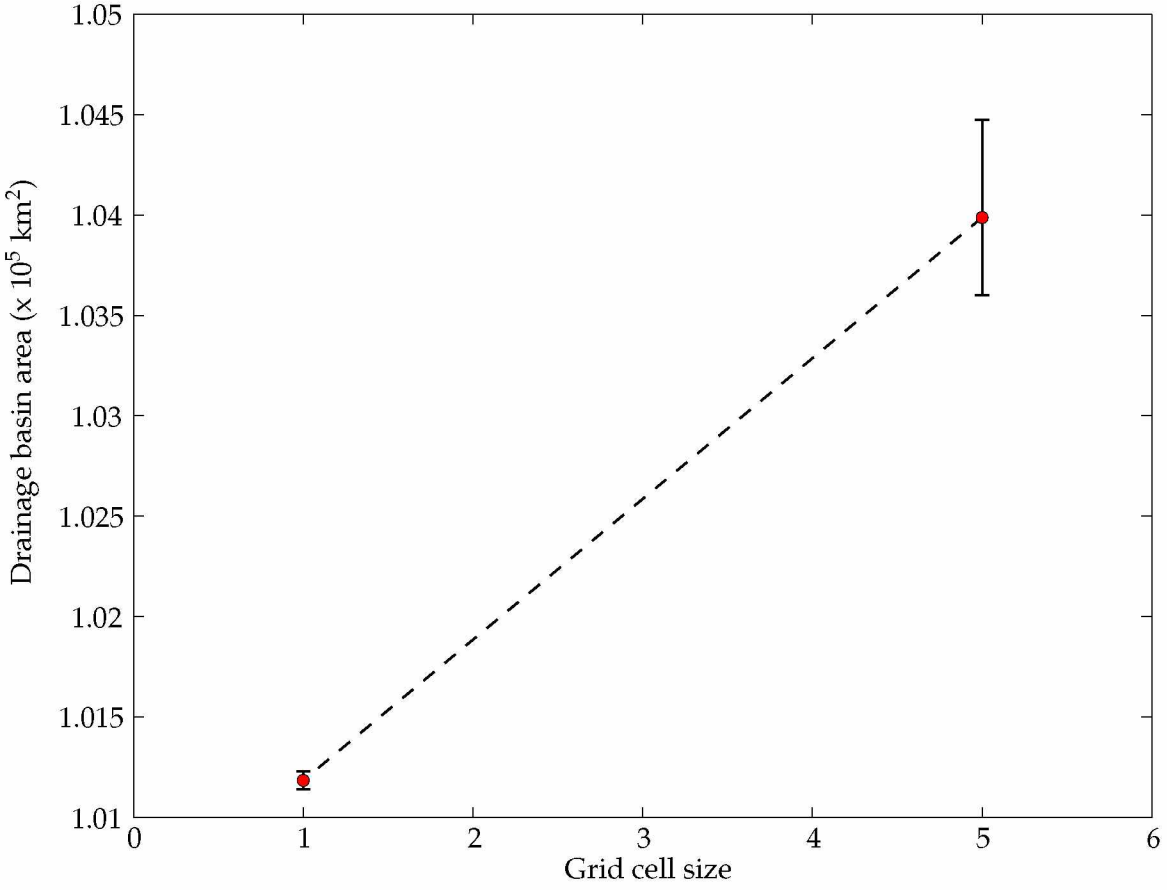

Figure 2.4. The average area of a drainage basin, for ten different runs of the generator, with respect to grid cell size. Here the error bars indicate the range of drainage basin areas determined by the generator, for $d = 5$ km and $N = 3$. Consecutive runs of the drainage basin generator with the same parameter values yield slightly different results because of the random element introduced by perturbing streamline origins. Although we only examined the dependence of basin area on grid cell size for 1 km and 5 km grids, ideally this plot will converge to the "true" area of the drainage basin as grid cell size approaches zero.

2.2.2 Boundary Conditions

PISM imposes periodic boundary conditions at the edge of the rectangular computational domain. For whole Greenland simulations, this is of no significance because no ice exists at that distance from the ice sheet. However, a periodic computational domain is not suitable for a regional model whose boundaries may be inside the ice sheet. Assigning the boundary values for the SIA, SSA, and energy balance equation in a regional ice sheet model (whose edges are within the ice sheet) is an inherently difficult task. These boundary values are nonzero and depend on the evolution of the entire ice sheet, which is neglected in a regional model. We make special considerations to assign boundary conditions.

In a narrow strip at the edge of the regional domain, we alter the computation of key quantities to provide constant domain boundary conditions in the model. The size of this strip is defined by the width of a single grid cell of the coarsest grid used during the spin-up procedure. In this narrow strip, referred to from here on as a "no-model strip" (NMS), we directly prescribe map-plane boundary values for ice thickness, surface elevation, enthalpy, basal melt, and SSA velocities or basal strength. The values for ice thickness, SSA sliding velocity, and enthalpy are then interpreted as Dirichlet boundary conditions at the internal boundary of the NMS by the SIA, SSA, and enthalpy field equations, respectively. See Figure 2.2.

Prior to running a regional simulation, we extract the three-dimensional enthalpy field, basal melt, and SSA velocity from a whole ice sheet simulation, and directly prescribe these to the NMS in the model. The edge of the domain (outside of the drainage basin) is typically characterized by slow-moving ice and prescribing low SSA velocities in the NMS prevents any sliding at the boundary. (Alternatively, basal strength may also be increased in the NMS to prevent sliding at the boundary.)

At the boundary, the surface gradient and driving stress calculations are modified to avoid differentiating an unphysical steep jump at the edge of the domain caused by the periodic boundary conditions. The regional model in PISM can alter the surface gradient and driving stress calculations in one of two ways. The first option involves setting the surface gradient in the NMS to zero, so that the driving stresses seen by the stress balance equations are zero. A second, more physically based option was used in this work. This option allows the regional branch of PISM to prescribe values of ice thickness and surface

elevation from a chosen ice sheet geometry to the NMS at the edge of the computational domain. These values are used to determine the surface gradient and driving stress at the boundary, and remain constant during a regional model run.

2.2.3 Force-to-thickness Mechanism

At the regional scale it is necessary to modify some of the assumptions that are made in a whole ice sheet model to separate the dynamics of a particular glacier from other fast-flowing basins. In particular, we assume that the regional domain area ice outside of the DB will stay near the present-day ice sheet geometry, while the area within the drainage basin dynamically evolves.

To isolate the dynamics of a specific catchment, we change the way we model ice outside of the DB. Specifically, a "force-to-thickness" (FTT) mechanism is applied to the area modeled outside of the DB, or the FTT area (Figure 2.2). This mechanism works by adding or ablating mass in order to offset ice thickness perturbations in the exterior ice. In the regional model, this mechanism is only applied to the slow-moving ice *outside* of the DB. Using the FTT, exterior ice is held near present-day thickness, and ice inside the DB is able to fully evolve according to the user-specified stress balance scheme (e.g. SIA, SSA, SIA+SSA hybrid). The resulting effect is the evolution of the ice at the interface between the outlet glacier and surrounding ice, while separating the dynamics of the outlet glacier from that of other catchments.

In detail, the FTT mechanism is a modification of the mass continuity equation:

$$\frac{\partial H}{\partial t} = M - S - \nabla_{x,y} \cdot \mathbf{q} \,. \tag{2.1}$$

Where H is the time-dependent ice thickness, M and S are the ice equivalent surface and basal mass balances, respectively, and $\mathbf{q}$ is map-plane ice flux. When using this mechanism, we let H_{tar} be the target present-day ice thickness *outside* of the drainage basin. The FTT mechanism causes M to be modified by a multiple of the difference between the target thickness and the current model thickness:

$$\Delta M = \gamma(H_{\text{tar}} - H), \tag{2.2}$$

where $0 < \gamma \leq 1$. We then add mass ($\Delta M > 0$) where $H_{\text{tar}} > H$ and ablate mass ($\Delta M < 0$)

where $H_{\text{tar}} < H$. This "forces" the ice modeled outside of the DB towards the present-day thickness by altering the surface mass balance (SMB).

The primary purpose of the FTT mechanism is to isolate the outlet glacier we have chosen to model from other fast flowing basins. However, this mechanism also prevents large surface gradients from occurring between the FTT area and the NMS. Although the only area of the regional domain that we are concerned with accurately modeling is the outlet glacier catchment, we still require that the FTT area and NMS maintain physical and consistent behavior during a simulation. An evaluation of whether or not results are physically reasonable is included in Chapter 4.

2.3 Modeling Choices

There are a number of physical parameters to explore in any numerical simulation. Previous work indicates that the recent acceleration of outlet glaciers in Greenland may be due to near-terminus changes which affect calving [21], [13] or enhanced basal lubrication from an increase in seasonal melt water reaching the bed [25] (although the latter may not be major a factor in outlet glacier acceleration [26]). Considering these mechanisms, we examine parameters which control the outlet glacier's basal resistance, calving style, and the ocean heat flux into the base of floating ice.

2.3.1 Basal resistance

PISM uses the shallow shelf approximation as a "sliding law" [17]. The basal resistance is described by a pseudo-plastic till. Specifically, stress at the base of the ice is a power law function of basal sliding velocity:

$$\tau_b = \tau_c \frac{|\mathbf{u}|^{q-1}}{u_{\text{threshold}}^{q}} \mathbf{u}. \tag{2.3}$$

Here τ_c is the positive scalar yield stress, $\mathbf{u}$ is the basal sliding velocity vector, q is a user-defined power, and $u_{\text{threshold}}$ is a user-defined velocity threshold. This model states that the till is able to support applied stresses without deformation, until the applied stress is equal to the yield stress, at which point deformation will occur. The purely plastic case ($q = 0$) is described in Schoof, 2006 [27]. In the linear case, where $q = 1$, the coefficient of velocity, $\tau_c/u_{\text{threshold}}$, is commonly called β or β^2 [28]. In this work we use a power of $q = 0.25$.

The yield stress for saturated till can be described by a Mohr-Coulomb relationship:

$$\tau_c = c_0 + \tan\phi(\rho g H - p_w), \tag{2.4}$$

where c_0 is the till cohesion (set to zero in this work [29]), ϕ is the till friction angle (a strength parameter for till), $\rho g H$ is the ice overburden pressure, and p_w is the pore water pressure. The difference between overburden and pore water pressure is the effective pressure of overlying ice on the saturated till.

The conservation of energy scheme generates basal melt water and this water is stored locally in the "till" at the base of the ice sheet [18]. Let W denote the effective thickness of this liquid water layer under the ice sheet. In a minimal hydrology model, water is added by the basal melt rate, subtracted by refreeze onto the base of the ice, and it drains away in the absence of other inputs according to a drainage parameter. The thickness W is updated at each time step according to these minimal models, but with additional spatial diffusion.

The water layer thickness W is involved in computing the basal water pressure ("pore water pressure") and thus the till yield stress. In lieu of a sophisticated subglacial hydrology model, we parameterize the pore water pressure so that, at most, it is a fixed fraction (α) of the overburden pressure,

$$p_w = (\alpha\rho g H)\frac{W}{W_0}, \tag{2.5}$$

where $0 \le W \le W_0$, and W_0 is the maximum thickness of this layer at 2 m (water above that level is lost in an unmodeled manner). This expression for pore water pressure allows for melt water to be stored locally in the till, where it is available to weaken till or for refreezing. When the base is frozen to the bed (i.e. $W = 0$) the pore water pressure will go to zero [17].

In this work, we examine how the regional model responds to changes in basal resistance by varying the allowed pore water pressure, α.

2.3.2 Calving Style

To explore model sensitivity to calving style, we examine three different calving mechanisms available in PISM. Earlier modeling efforts of outlet glaciers demonstrate that boundary conditions at the terminus play the most significant role in glacier dynamics [13]. In particular, Amundson and Truffer [30] show that calving rate is, to first order, controlled

by ice thickness, thickness gradient, strain rate, mass balance, and backward melting of the terminus. Each of the following calving mechanisms were used to examine model sensitivity:

2.3.2.1 Calving Floating Ice

The first calving style simply removes any ice that satisfies the flotation criterion. Using the "float kill" mechanism all floating ice is immediately calved off and there are no ice shelves in the model. This treatment oversimplifies the calving process of many glaciers, but it may be appropriate for modeling the retreat of Jakobshavn. Observations indicate that calving of grounded ice is difficult, providing a good argument for flotation related calving [21].

2.3.2.2 Calving Ice at Present-day Calving Front

This calving style is based on the mask values that are provided at the beginning of a model run. Any locations which were ice-free ocean at the beginning of the run are places where floating ice is removed. Specifically, all ice shelves (floating tongues) are calved off at the location of the present-day glacier terminus.

2.3.2.3 Eigen-Calving at Thickness

The physically based "eigen-calving" 2D-calving parameterization is developed in [31]. The parameterization assumes that average calving rates, c, are proportional to the product of principal components of the horizontal strain rates, $\dot{\varepsilon}_{\pm}$, which are derived from SSA-velocities,

$$c = k\,\dot{\varepsilon}_{+}\,\dot{\varepsilon}_{-} \quad \text{and} \quad \dot{\varepsilon}_{\pm} > 0\,. \tag{2.6}$$

Here, the constant k is related to the material properties of the ice at the calving front. The actual strain rate pattern depends on the geometry and boundary conditions at the margins of the ice shelf (e.g. coastlines, ice rises, or front position). This pattern provides information about areas where preexisting fractures are likely to grow and form rifts (in two directions). If these rifts intersect, they can lead to the release of icebergs. The eigen-calving style, however, is not intended to resolve individual rifts or calving events;

this first-order approach produces structurally-stable calving front positions and has been shown to agree with observations [31].

When using this mechanism, the calving rate is proportional to the product of principal strain rates, where they are positive. Additionally, ice is removed when it becomes thinner than a user-specified thickness H_0, at a rate at most one grid cell per time step. A partially-filled grid cell formulation [32] provides a framework to relate the eigen-calving rate to the mass transport scheme at the ice shelf terminus. Ice shelf front advance and retreat due to calving are limited to a maximum of one grid cell length per time step.

2.3.3 Sub-shelf Ocean Heat Flux

Since boundary conditions at the terminus may play the most crucial role in glacier acceleration, we examine an additional parameter in experiments that support a moving glacier terminus and build-up of a floating tongue (i.e. eigen-calving model runs). Amundson, et al. [21] suggest that calving rate, which controls the extent of the floating tongue, is also influenced by seasonal changes in the outlet glacier fjord, such as seawater temperature and the amount of sea ice. This implies that outlet glaciers are dynamically sensitive to changes that are coupled to air and ocean conditions. Additionally, observations indicate that the acceleration of the Jakobshavn Isbræ was triggered by an increase in subsurface oceans temperature in Disko Bay [33]. Motyka et al. [34] show that a measured 1.1°C increase in water temperature in Disko Bay is sufficient to explain the observed thinning of Jakobshavn's floating tongue prior to its breakup, if a linear relationship between thermal forcing and melting is assumed. Therefore, in experiments which allow a floating tongue to develop, we vary the amount of sub-shelf ocean heat flux into the ice.

Chapter 3
Results

3.1 The Jakobshavn Regional Ice Sheet Model

PISM and the regional modeling tools were applied to a regional model of the Jakobshavn Isbræ. Jakobshavn is the most active outlet glacier in Greenland and drains about 5% of the ice sheet area [9]. Modeling the entire Greenland ice sheet (1,800,000 km^2) has been performed, but with resolution limitations (e.g. 5 km grid cell spacing). Considering only the area of the Jakobshavn Isbræ catchment (110,000 km^2), however, has allowed us to examine this region at unprecedented resolutions (e.g. 1 km grid cell spacing).

In the following sections we prescribe surface, basal, and domain boundary conditions.

3.1.1 Modeling Input

A summary of the regional model components and inputs is included in Table 3.1.

We do not attempt to model the surface melt processes, or distinguish between precipitation as rain or snow. Instead, we directly supply the surface mass balance (SMB) to our ice dynamics model using results from the HIRHAM regional atmospheric climate model [35]. HIRHAM is developed jointly by the Danish Meteorological Institute and the Max-Planck Institute. The model has been applied to Greenland to examine climate variability and change on a regional scale for the 1989 to 2009 time period. In this work, we use a highly simplified surface mass balance scheme and only apply the 1989 annual SMB to the Jakobshavn regional model.

Measurements of ice thickness, ice surface elevation, land elevation in ice free areas, and bedrock topography were used from Bamber and others (2001) [1]. These fields also incorporated updated and corrected 5 km gridded data from the National Snow and Ice Data Center (NSIDC), bathymetric data and surface elevation data for Ellesmere Island from the General Bathymetric Chart of the Oceans (GEBCO), and gridded flightline data for the Jakobshavn region from the Center for Remote Sensing of Ice Sheets (CReSIS) [23]. In this work, we refer to this combination of datasets as the "present-day" ice sheet geometry.

The Shapiro and Ritzwoller [36] data set for geothermal flux was used as a basal boundary condition. This field was applied to the base of of the bedrock layer. The smoothly-

varying map lacked small-scale features, therefore this work was not influenced by geothermal spatial variations.

We extract the regional model boundary conditions for enthalpy, basal melt, and SSA velocity from a whole Greenland ice sheet model run at 5 km spatial resolution. The whole Greenland run was conducted using the polythermal SIA+SSA hybrid scheme, paleoclimate forcing, and was run for 125,000 years. Boundary conditions for ice thickness and ice surface elevation were taken from the present-day ice sheet geometry. These boundary conditions remained fixed in each regional model experiment.

Table 3.1. Regional model components and inputs.

Grid sizes	5 km, 2 km, 1 km
Surface mass balance	HIRHAM regional atmospheric climate model [35].
Bedrock topography	Bamber et al., 2001 [1] and CReSIS flightline data for Jakoshavn [23].
Geothermal heat flux	Shapiro and Ritzwoller, 2004 [36]
Stress balance	SIA+SSA hybrid [17]

3.2 Experiments

The model runs presented here were conducted using computer resources at the University of Alaska Geophysical Institute and the Arctic Region Supercomputing Center in Fairbanks, Alaska. Each parameter experiment in this work was completed on a 2080-processor Penguin Computing Cluster. The computational cost was an average of 445 and 2070 processor hours for the 2 km and 1 km model runs, respectively.

A model spin-up run (see Figure 3.1) was completed to achieve the initial enthalpy field. The spin-up used 1989 surface mass balance model results from HIRHAM and a present-day initial geometry. The initial enthalpy field was generated by first completing a 50,000 year SIA run on a fixed geometry (e.g. no surface change) to achieve approximate enthalpy equilibrium on a 5 km grid. The SIA-only run was followed by a 50,000 year SIA+SSA hybrid model run, which allowed for an evolving upper surface, and was conducted with a 5 km to 2 km to 1 km grid refinement. The spin-up was completed using the base parameter set ($\alpha = 0.98$, calving at the present-day calving front, and an ocean heat flux of $Q = 0.5$ W m^{-2}).

A parameter study was conducted to determine the modeling choices (basal water pressure, calving style, and ocean heat flux) that best capture the dynamics of the Jakobshavn Isbræ. A total of fifteen experiments were completed to examine the effect of different parameter combinations. Specifically, this parameter study was performed in two parts (see Figure 3.1). The first part of the study focused on the effects of calving style in the regional model while using a constant default value for Q, the sub-ice shelf heat flux into the ice. While holding this modeling parameter at a constant value (Q = 0.5 W m^{-2}), we changed the calving style to determine which style best represents the present-day behavior of Jakobshavn. In the second part of the study we varied Q to examine how temperature changes in ocean water will affect the floating tongue. This part of the study was only applicable to model runs which allowed the development of a floating tongue at Jakobshavn by using the eigen-calving style. In each part of the study α, the allowed pore water pressure, was adjusted to investigate the effect basal sliding in experiments.

To allow the parameter choices for each experiment to influence the model after the spin-up, we ran each experiment 1,000 years on a 2 km grid. A total of fifteen experiments were completed at a resolution of 2 km. From these experiments the best parameter combinations were identified, and runs with these model choices were then continued for 100 model years on a 1 km grid to express results at high resolution (See Figure 3.1).

3.3 Model Validation

In order to validate results produced by the regional model, model runs were compared to spatially-rich SAR observed surface speed data [22] and the present-day geometry of the Jakobshavn region [1], [23]. A direct comparison between observed and modeled surface speeds and ice thickness was conducted for each experiment (see Figure 3.1), and the absolute (Abs.) mean and root-mean square (RMS) differences were calculated. These values are outlined for the 2 km study in Tables 3.2-3.5. The best model results (those which differed the least from the observed) are highlighted in each table.

Tables 3.2 and 3.3 outline the comparison between modeled and observed ice surface speeds and thickness for the first part of the study, which focused on the influence of calving style. For this direct comparison, the experiment with α = 0.98, and an ocean-kill calving style is the most consistent with observed values of surface speed. When directly

compared with observed values of ice thickness, however, model results with pore water pressure $\alpha = 0.95$ appear most accurate for both the ocean-kill and float-kill calving styles. The presence of a floating tongue in all eigen-calving experiments generated fast-flowing ice in present-day ice free areas of the fjord, therefore a direct comparison between modeled and observed values may be less relevant for model runs where a floating tongue develops.

In the second part of this study, we focused on the influence of Q, the heat flux into the ice, and its effect on the development of a floating tongue in the model; the results are outlined in Tables 3.4 and 3.5. Model results using the low values of ocean heat flux ($Q \leq 1.0\ \mathrm{W\ m^{-2}}$) consistently developed a floating tongue at the Jakobshavn Isbræ regardless of the pore water pressure. Increasing the value of Q improved model results by limiting the development of an ice shelf. Specifically, experiments which used a pore water pressure $\alpha = 0.95$ and large values for heat flux produced the best results when directly compared observed values of both surface speed and thickness.

After appropriately identifying parameter combinations which produced good results relative to observations, we continued these simulations at high resolution (1 km grid cell spacing) to examine how improvements in resolution alter these results. Three experiments were identified, and their results are summarized in Tables 3.6 and 3.7. Specifically, these three experiments were chosen because they represented the best results (according to direct comparisons) for either the calving style or heat flux studies. The 1 km model run which used the float-kill calving style and $\alpha = 0.95$ produced the best results when compared to the observed values for both ice thickness and surface speed. The 1 km model results, overall, showed improvement with respect to ice thickness (except for the eigen-calving), but not surface speed. A map-plane comparison between observed and modeled results is shown in Figure 3.1.

Errors or the absence of information in some model inputs (e.g. bedrock topography or basal strength) may mis-locate the fast-flowing features in the regional model. Therefore, it is also relevant to compare the *distribution* of surface speeds for modeled and observed results. Figures 3.2 and 3.3, illustrate the distribution surface speeds for the observed values as well as the best 2 km parameter model results; results from an SIA-only run (i.e. no basal sliding) are also shown for comparison. A logarithmic vertical scale emphasizes

differences in the amount of fast flow for each experiment. The results of this histogram indicate that the ocean-kill run with $\alpha = 0.98$ best captures the over distribution of ice surface speeds.

Table 3.2. Velocity comparison for 2 km calving-style study.

Parameter experiment	**RMS difference (m a^{-1})**	**Abs. mean difference (m a^{-1})**
$\alpha = 0.95$, Eigen	249.50	48.20
$\alpha = 0.98$, Eigen	241.40	47.70
$\alpha = 0.99$, Eigen	265.80	50.00
$\alpha = 0.95$, Float	171.70	37.50
$\alpha = 0.98$, Float	175.40	44.60
$\alpha = 0.99$, Float	191.90	61.30
$\alpha = 0.95$, Ocean	172.00	37.60
$\alpha = 0.98$, Ocean	159.60	44.90
$\alpha = 0.99$, Ocean	192.40	61.40

Table 3.3. Geometry comparison for 2 km calving-style study.

Parameter experiment	**RMS difference (m)**	**Abs. mean difference (m)**
$\alpha = 0.95$, Eigen	68.70	26.30
$\alpha = 0.98$, Eigen	78.00	31.00
$\alpha = 0.99$, Eigen	66.40	41.40
$\alpha = 0.95$, Float	53.20	32.00
$\alpha = 0.98$, Float	97.50	69.70
$\alpha = 0.99$, Float	162.30	127.30
$\alpha = 0.95$, Ocean	53.20	32.00
$\alpha = 0.98$, Ocean	89.50	63.50
$\alpha = 0.99$, Ocean	162.30	127.30

Table 3.4. Velocity comparison for 2 km ocean heat flux study.

Parameter experiment	RMS difference (m a^{-1})	Abs. mean difference (m a^{-1})
$\alpha = 0.95, Q = 0.5$	249.50	48.20
$\alpha = 0.98, Q = 0.5$	241.10	47.70
$\alpha = 0.99, Q = 0.5$	265.80	59.10
$\alpha = 0.95, Q = 2.5$	189.00	39.00
$\alpha = 0.98, Q = 2.5$	244.30	47.70
$\alpha = 0.99, Q = 2.5$	266.30	59.50
$\alpha = 0.95, Q = 10.0$	189.00	39.00
$\alpha = 0.98, Q = 10.0$	243.40	47.00
$\alpha = 0.99, Q = 10.0$	265.50	59.20

Table 3.5. Geometry comparison for 2 km ocean heat flux study.

Parameter experiment	RMS difference (m)	Abs. mean difference (m)
$\alpha = 0.95, Q = 0.5$	68.70	26.30
$\alpha = 0.98, Q = 0.5$	78.00	31.00
$\alpha = 0.99, Q = 0.5$	66.40	41.40
$\alpha = 0.95, Q = 2.5$	46.90	25.50
$\alpha = 0.98, Q = 2.5$	76.50	29.70
$\alpha = 0.99, Q = 2.5$	72.80	53.00
$\alpha = 0.95, Q = 10.0$	46.90	25.50
$\alpha = 0.98, Q = 10.0$	76.70	29.60
$\alpha = 0.99, Q = 10.0$	65.00	43.40

Table 3.6. Velocity comparison for 1 km parameter study.

Parameter experiment	**RMS difference (m a^{-1})**	**Abs. mean difference (m a^{-1})**
α = 0.95, Q= 2.5, Eigen	273.70	50.80
α = 0.95, Q= 0.5, Float	172.30	37.00
α = 0.98, Q= 0.5, Ocean	172.90	46.40

Table 3.7. Geometry comparison for 1 km parameter study.

Parameter experiment	**RMS difference (m)**	**Abs. mean difference (m)**
α = 0.95, Q= 2.5, Eigen	74.20	28.00
α = 0.95, Q= 0.5, Float	58.60	34.00
α = 0.98, Q= 0.5, Ocean	89.90	68.00

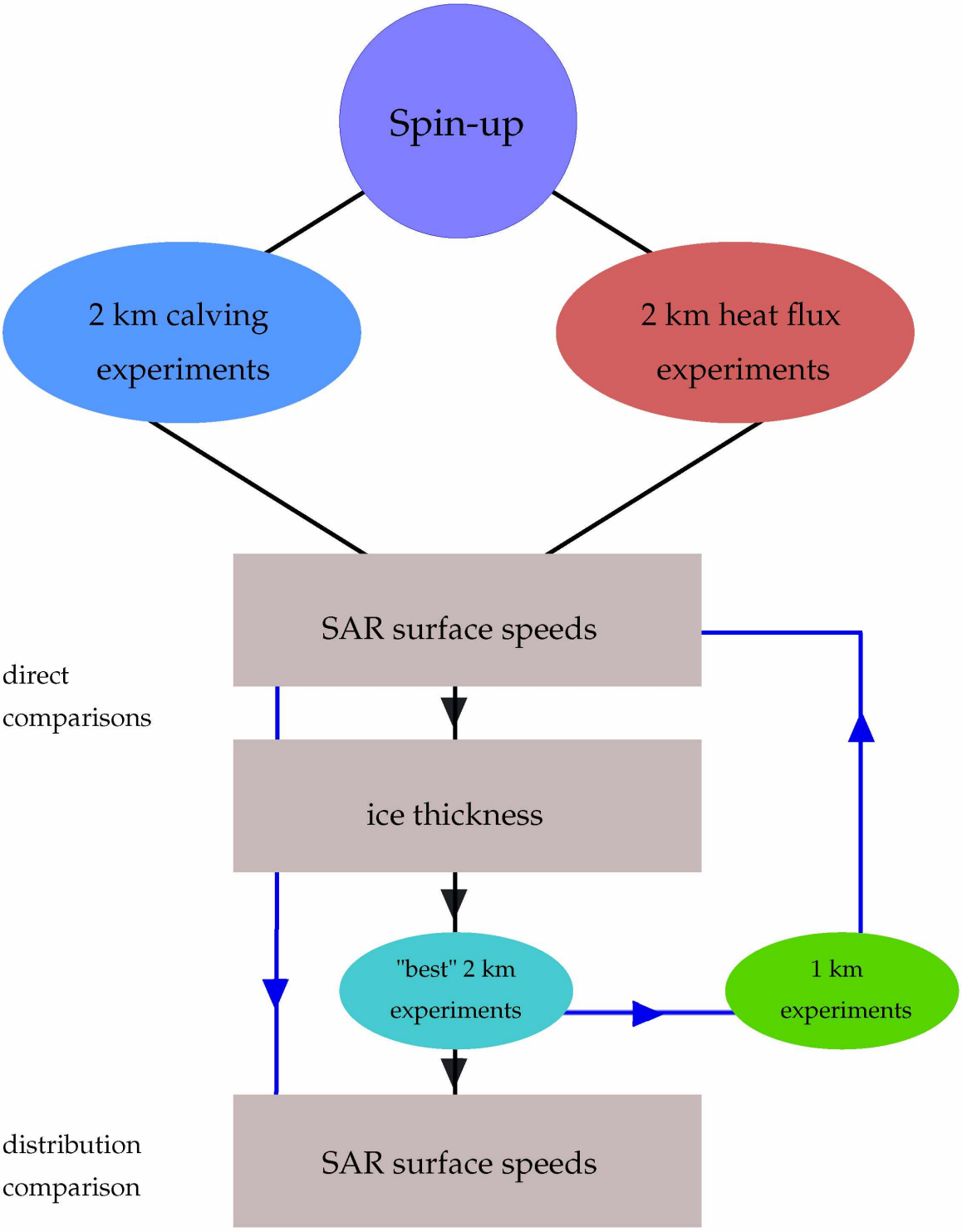

Figure 3.1. A flowchart that depicts the procedure used to generate and validate all of the model results in this parameter study.

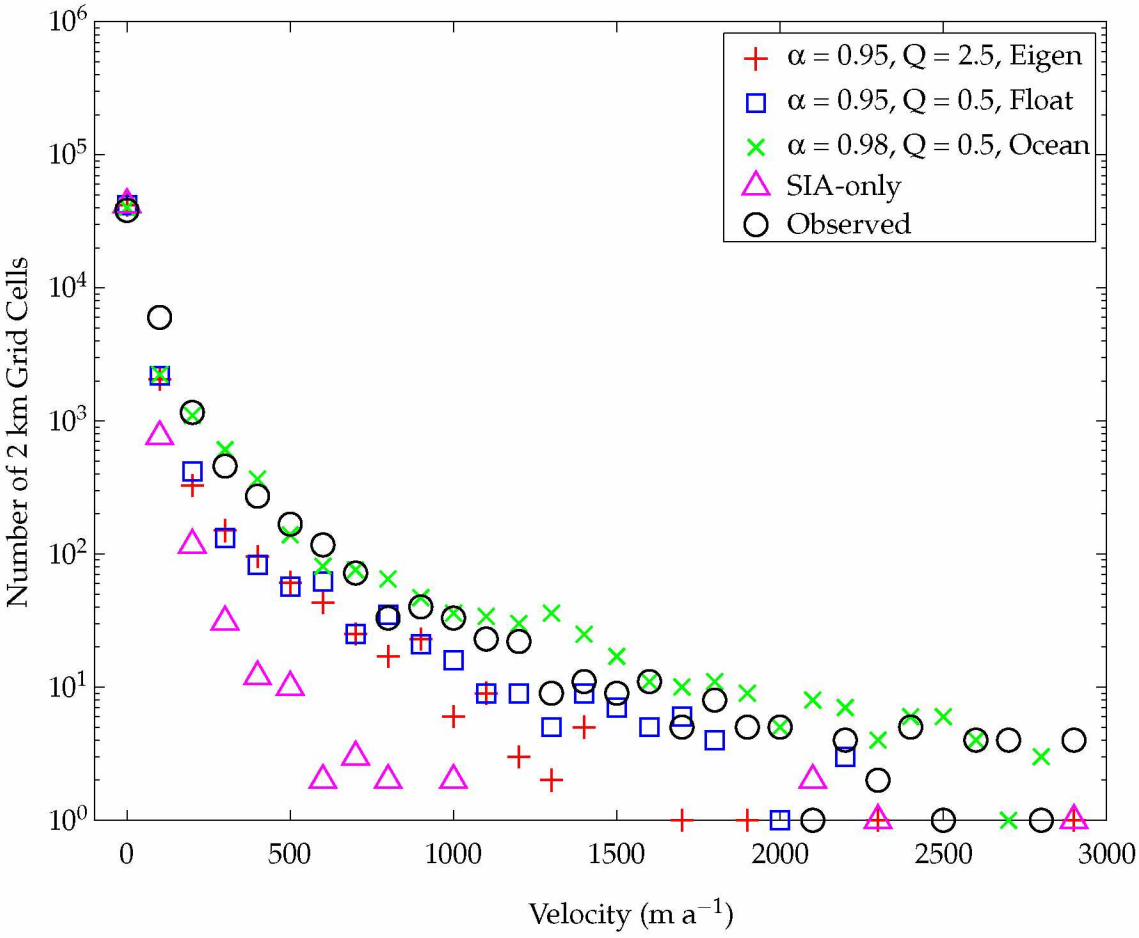

Figure 3.2. Distribution of modeled and observed surface speeds for 2 km experiments.

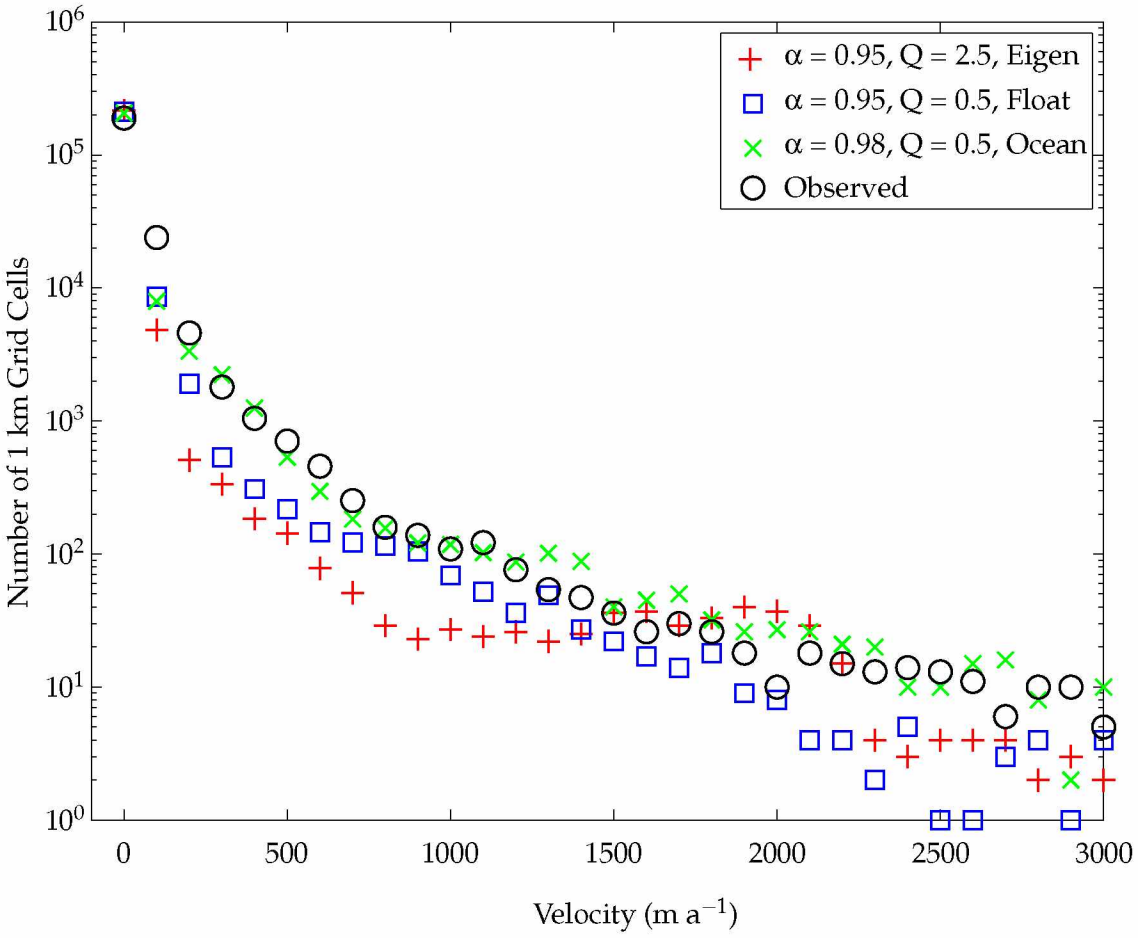

Figure 3.3. Distribution of modeled and observed surface speeds for 1 km experiments.

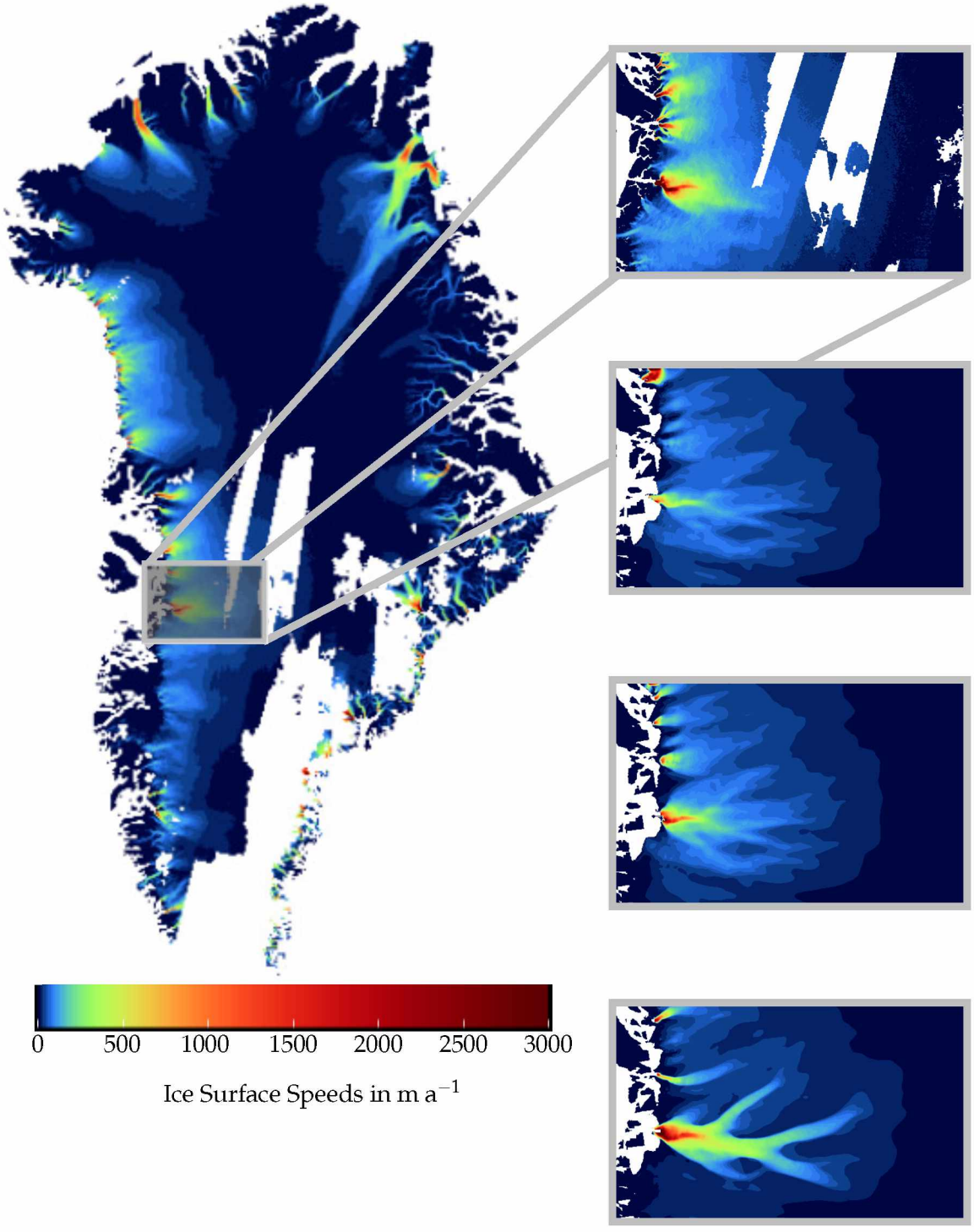

Figure 3.4. Map-plane view of modeled and observed surface speeds for 1 km experiments. (From top to bottom) Observed, Eigen-calving, Float-kill, and Ocean-kill surface speeds.

Chapter 4
Discussion and Conclusions

4.1 Performance

We have conducted a parameter study to examine how the regional model reacts to three important model parameters: allowed pore water pressure, calving style, and ocean heat flux. The purpose of this study was not to produce a model that closely matches the observations, but rather to identify sets of parameters that cause a given behavior within the model. Regardless, the 2 km parameter study does demonstrate the ability of the model to nearly match observed velocity distributions. This confirms that we have identified a subset of the model parameter space that is suitable for capturing the dynamics of an ice sheet region. Figure 3.3 illustrates the improvements that are achieved by using the leading-order SIA+SSA hybrid scheme over an SIA-only model. The SIA-only model substantially overestimates the amount of slow moving ice ($\leq$ 100 m a^{-1}) and considerably underestimates the amount of medium and fast flowing ice (>100 m a^{-1}). This indicates that an SIA-only model is *not* appropriate for a regional model of the Jakobshavn Isbræ.

Increasing the resolution from 2 km to 1 km in the parameter study did not show model improvement with respect to ice thickness or surface speed. Potentially, this is a consequence of the lack of information at the basal boundary, which can misplace the fast-flowing features in an ice sheet model. For example, if errors in a bedrock topography map mis-locate a deep channel, the ice dynamics will reflect this and also mis-locate the velocities generated by the high driving stresses in the channel. To account for this, we examine the model with respect the the distribution of observed surface speeds at 1 km. At high resolution, the performance of model results is mixed when compared to the observed distribution of slow- and medium-flowing ice. However, all model runs showed improvement with increased resolution for estimates of fast-flowing ice. This is due the ability of a higher resolution model to resolve important small-scale features in topography that produce fast-flow in the region (e.g. the deep bed rock channel under Jakobshavn). The ocean-kill run with a pore-water pressure of $\alpha = 0.98$ best matched the observed surface speed distribution for both the 2 km and 1 km parameter experiments.

At high resolution, model runs which used the float-kill or ocean-kill calving styles outperform eigen-calving runs. This is demonstrated when model results are compared

directly to observations of geometry and surface speed, and to the distribution of surface speeds. These results are consistent with observations that calving of grounded ice is difficult at the present-day terminus of the Jakobshavn Isbræ [21]. This does not imply that the simplified calving styles are superior to the more physically based eigen-calving mechanism. Instead, it indicates that the eigen-calving choice is not suitable for a model that aims to reproduce the *current* behavior at the Jakobshavn Isbræ. The eigen-calving style will be most appropriate in model runs that attempt to capture earlier behavior of the Jakobshavn Isbræ (e.g. prior to the disintegration floating tongue in 1998 [34]).

Interesting behavior was observed for the eigen-calving runs in the context of the ocean heat flux study and at high resolution. For all eigen-calving runs that developed a floating tongue, the modeled volume of floating ice was close to the observed values, on the order of 10^9 m^3. Despite this, the model did not produce comparable melt rates to those which lead to the break up of the floating tongue at Jakobshavn. For the model run $\alpha = 0.95$ and $Q = 0.5$ W m^{-2} the maximum submarine melt rate was calculated to be approximately 2 m a^{-1}, and for $\alpha = 0.95$ and $Q = 1$ W m^{-2} the it was determined to be around 0.6 m a^{-1}. By comparison, melt rates on the order of 200 m a^{-1} were observed prior to the break up of Jakobshavn's floating tongue [34].

The ability of the model to create a floating tongue of comparable volume to the observed tongue is a promising result and demonstrates the potential of the eigen-calving mechanism. However, a large discrepancy between the modeled and observed melt rates implies that the model does not properly account for the way in which mass is lost. This seems to indicate that the regional model overestimates the ice that is lost to calving while underestimating ice lost to submarine melting. It may also suggest that there is fundamental problem in the way PISM determines the ice flux across the grounding line.

4.2 Capability of the PISM Regional Model

The PISM regional model is analogous to a nested ice sheet model. Nested models are achieved by either "one-way" or "two-way" methods. In one-way nesting, the coarse-resolution domain simulation is run independently of a higher-resolution subset of the domain, or a "nest". That whole domain then provides the initial and boundary conditions for the nest domain. There are no feedbacks between the coarse domain and its nest in

one-way nesting, and simulated behavior at the same grid point in the coarse-resolution domain is often slightly different from that in the one-way nest. In PISM, we do not perform actual grid nesting to avoid a timestep restrictions from the Courant-Friedrichs-Lewy (CFL) number. The CFL number, and subsequent timestep restriction determined by PISM, consider both high spatial resolution and the velocity of ice advection. If a nested grid is implemented, the whole ice sheet model and the regional (nested) model may decrease the computational efficiency of one another. In the regional domain, however, a user can specify the initial and boundary conditions provided by the whole-ice sheet domain, much like a true one-way nested model.

Because this work is similar to a one-way nested model, it is important to evaluate the duration for which the model is relevant after initialization, or the "temporal resolution". In this context, we do not refer to temporal resolution as the minimum possible time-step achieved in the regional model, but rather to the duration at which the simulation is able to accurately model an outlet glacier without updating the domain boundary conditions.

To investigate the temporal resolution of the regional model, we perturb ice both inside and outside of the drainage basin and examine how long it takes these perturbations to reach the terminus or domain boundary. It is important to perturb the model in such a way as to not impact the ice dynamics we want to examine. Therefore we alter the three dimensional ice age field, as the age attribute will advect through the ice during a simulation, but does not affect ice dynamics in PISM. Specifically, we set ice in the whole computational domain to an age of 0 model years, and then modify the age of two columns of ice; one inside of the the drainage basin and another outside of the basin. By setting two columns of ice age to different values, which are orders of magnitude larger than the background age, we can use old ice as a tracer in the model. This allows us to examine how ice moves through the model domain in the x, y, and z directions.

In particular, we performed a 5 km SIA+SSA run for 1000 model years to map the advection of ice in the regional domain both in and outside of the drainage basin. Inside the drainage basin we examine a column of ice that is near the eastern edge of the basin margin. This first age-tracer (AT1) flows through the drainage basin to the glacier terminus; by the end of the model run some of the ice in AT1 has exited the Jakobshavn Isbræ, and some remains near the glacier terminus. The second age-tracer (AT2) is a column of ice

near the eastern divide in an area between the DB and NMS, where the FTT mechanism is applied. AT2 exhibits very slow flow, only about 15 km during the 1000 year model run. Additionally, AT2 ice does not exit through the domain boundary nor does it enter the drainage basin. See Figure 4.1.

From this short experiment, we note two important outcomes. First, ice that is modeled in an unphysical way outside of the drainage basin (using FTT) does not enter the drainage basin on the order of a millennium. Second, perturbations that occur within the drainage basin appear to be confined to the drainage basin and do not affect the domain boundaries where we have prescribed boundary conditions from a whole-ice sheet model. This suggests that the results of a PISM regional model of Jakobshavn are relevant for at least 1000 model years after initialization. It also indicates that this model is suitable for 100-200 year forecasting runs which aim to predict the ice sheet sea level contribution, such as those conducted by the Sea-level Response to Ice Sheet Evolution (SeaRISE) Assessment [37].

4.3 Future Work

In the regional model we directly supply the results from a separate atmospheric model, HIRHAM, as the SMB boundary condition. We then use the 1989 annual mean SMB and apply it every model year during both the spin-up and parameter study runs. Although this is a simplified model, it may be appropriate for the spin-up stage (when allowing the ice to achieve a thermal steady state over several thousand model years) and the parameter study (when the goal is to explore a subset of the model parameter space). In model runs that are evaluated relative to observations, however, this SMB scheme may lack the temporal resolution and variability needed to accurately capture the observed behavior. Future work includes a high resolution Jakobshavn regional model which uses the monthly mean SMB results from HIRHAM to model the dynamics of the glacier during the entire 1989 to 2009 period.

Because it is inherently difficult to obtain large-scale direct measurements at the base of an ice sheet, specifying basal boundary conditions remains a significant challenge in ice sheet modeling. In this work, we relate the basal strength to an elevation dependent material strength, motivated by the hypothesis that low-lying areas with a marine history

should be weak. We plan to improve the determination of basal strength using widely available surface velocity measurements. A classical ill-posed problem exists when boundary conditions are abundant at one boundary and not sufficient at another. This ill-posed problem can be solved using inverse methods, and a basal strength field can be constructed by fitting modeled to observed surface velocities. In the future, PISM will infer the basal strength from surface velocity measurements using an iterative inverse method [38].

Bedrock topography for the Jakobshavn region is taken from gridded flightline data released by CReSIS in 2010 [23]. Although this dataset represents the most recent and highest resolution information available about the bedrock topography at Jakobshavn, it still contain inconsistencies and data processing artifacts. Efforts are underway to address these problems and improve the dataset. Recently, the Ice2Sea Collaboration released a new version of this bed map, which will be used in future regional models.

Additionally, most future work will take place at higher resolution than what is presented here. We plan to run the model at higher resolutions ($\leq$500 m grid cell spacing) to further resolve important small-scale features, such as the trunk of Jakobshavn (~5 km in width) or the floating ice tongue (~3 km in width).

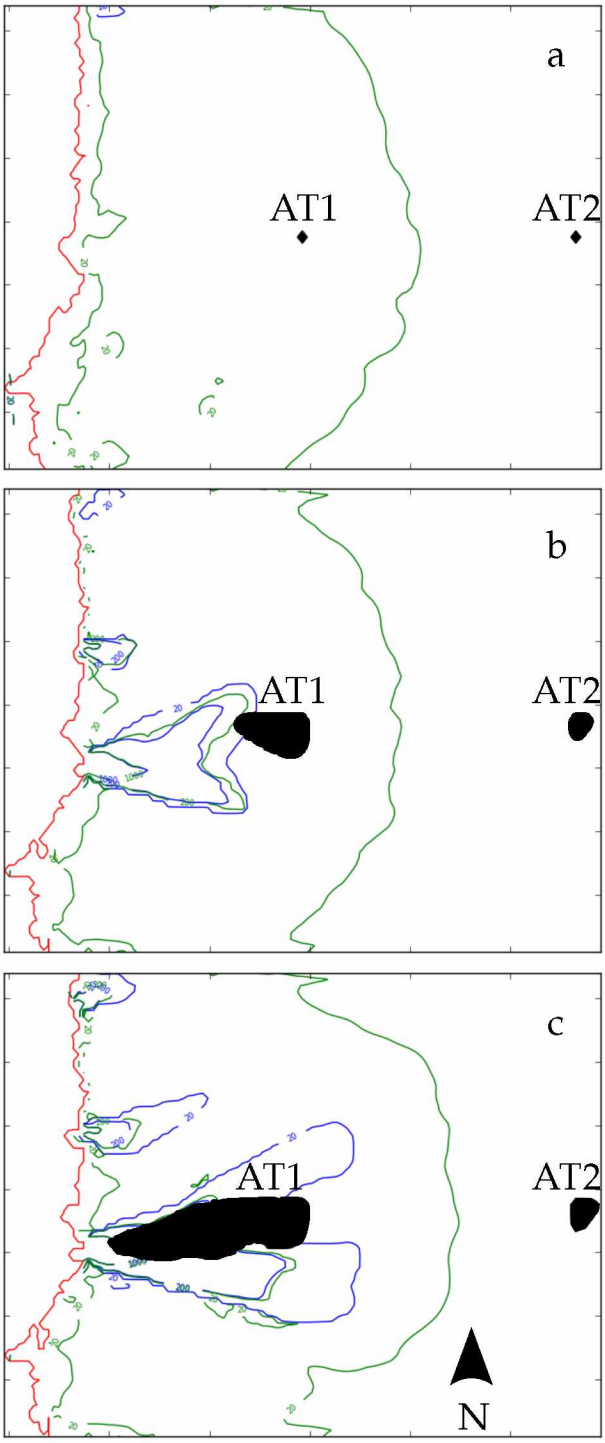

Figure 4.1. Snapshots of the the age-tracer experiment at (a) 0 model years, (b) 500 model years, and (c) 1000 model years. Here red indicates the position of the coastline, blue and green represent the surface speeds and basal speeds, respectively (m a $^{-1}$), and black indicates areas of old ice. Courtesy of Constantine Khroulev.

Chapter 5
Conclusions

Although the model described here was developed for the purpose of ice sheet modeling, this work addresses some principal challenges associated with the numerical simulation of physical systems. Our aim was to take a large-scale dynamic system (an ice sheet) and focus in on smaller region of that system at high resolution (an outlet glacier), and then examine how this region evolves independently with time. To perform this work we had to first address some fundamental questions: What area is suitable for this model domain? How should we prescribe boundary conditions? For what timescales, and to what degree, does the regional model evolve independently? Because ice sheet modeling at the regional scale is a recent advance in the glaciological community, it was necessary to develop novel techniques to address these questions. Specifically, we created a drainage basin generator algorithm to identify outlet glacier catchments and define a regional domain. We then developed a method to specify the appropriate map-plane boundary values and Dirichlet boundary conditions to the key equations in this model (SIA, SSA, and enthalpy field equation). Finally, we determined an appropriate way to modify the dynamics outside of the drainage basin to isolate the glacier in the model. After developing these techniques and creating the regional model, it was essential to validate the results against glaciological observations to ensure that we are indeed capturing the underlying physics.

This model presented in this work is best suited for simulating a region of an ice sheet at high spatial resolutions ($\leq$1 km) and on short timescales ($\leq$1000 a). These resolutions and timescales are adequate for sea level rise forecasting. Because the largest uncertainty in constraining sea level contribution from Greenland lies in the ability of a model to capture changes in the outlet systems [10], we intend for this model to be used as a tool to help constrain sea level contribution from outlet glaciers. Additionally, these regional modeling tools are now part of PISM, and therefore add to the publicly available ice sheet modeling software.

Bibliography

[1] J. Bamber, R. Layberry, and S. Gogineni. A new ice thickness and bed data set for the Greenland ice sheet. I- measurement, data reduction, and errors. *Journal of Geophysical Research*, 106:33, 2001.

[2] M.B. Lythe, D.G. Vaughan, and The BEDMAP Group. BEDMAP: A new ice thickness and subglacial topographic model of Antarctica. *Journal of Geophysical Research*, 106:11335–11351, 2001.

[3] M.F. Meier, M.B. Dyurgerov, U.K. Rick, S. O'Neel, W.T. Pfeffer, R.S. Anderson, S.P. Anderson, and A.F. Glazovsky. Glaciers dominate eustatic sea-level rise in the 21st century. *Science*, 317(5841):1064, 2007.

[4] R.B. Alley, M.K. Spencer, and S. Anandakrishnan. Ice-sheet mass balance: assessment, attribution and prognosis. *Annals of Glaciology*, 46(1):1–7, 2007.

[5] H.D. Pritchard, R.J. Arthern, D.G. Vaughan, and L.A. Edwards. Extensive dynamic thinning on the margins of the Greenland and Antarctic ice sheets. *Nature*, 461(7266):971–975, 2009.

[6] S. Rahmstorf, A. Cazenave, J.A. Church, J.E. Hansen, R.F. Keeling, D.E. Parker, and R.C.J. Somerville. Recent climate observations compared to projections. *Science*, 316(5825):709, 2007.

[7] R.K. Pachauri. *Climate Change 2007: Synthesis Report*. IPCC Secretariat, 7 bis Avenue de la Paix C. P. 2300 Geneva 2 CH- 1211 Switzerland, 2008.

[8] J.L. Bamber, D.G. Vaughan, and I. Joughin. Widespread complex flow in the interior of the Antarctic ice sheet. *Science*, 287(5456):1248, 2000.

[9] E. Rignot and P. Kanagaratnam. Changes in the velocity structure of the Greenland ice sheet. *Science*, 311(5763):986, 2006.

[10] M. Truffer and M. Fahnestock. Rethinking ice sheet time scales. *Science*, 315(5818):1508, 2007.

[11] J.M. Amundson, M. Truffer, M.P. Lüthi, M. Fahnestock, M. West, and R.J. Motyka. Glacier, fjord, and seismic response to recent large calving events, Jakobshavn Isbræ, Greenland. *Geophysical Research Letters*, 35:22, 2008.

[12] I. Joughin. Ice-sheet velocity mapping: a combined interferometric and speckle-tracking approach. *Annals of Glaciology*, 34(1):195–201, 2002.

[13] F.M. Nick, A. Vieli, I.M. Howat, and I. Joughin. Large-scale changes in Greenland outlet glacier dynamics triggered at the terminus. *Nature Geoscience*, 2(2):110–114, 2009.

[14] B.R. Parizek and R.T. Walker. Implications of initial conditions and ice-ocean coupling for grounding-line evolution. *Earth and Planetary Science Letters*, 300:351–358, 2010.

[15] G. Durand, O. Gagliardini, L. Favier, T. Zwinger, and E. le Meur. Impact of bedrock description on modeling ice sheet dynamics. *Geophysical Research Letters*, 38(20):L20501, 2011.

[16] C.S. Lingle and E.N. Troshina. Relative magnitudes of shear and longitudinal strain rates in the inland Antarctic ice sheet, and response to increasing accumulation. *Annals of Glaciology*, 27:187–193, 1998.

[17] E. Bueler and J. Brown. Shallow shelf approximation as a sliding law in a thermomechanically coupled ice sheet model. *Journal of Geophysical Research*, 114(F3):F03008, 2009.

[18] A. Aschwanden, E. Bueler, C. Khroulev, and H. Blatter. An enthalpy formulation for glaciers and ice sheets. *Journal of Glaciology*, 2011. Submitted.

[19] K. Echelmeyer, TS Clarke, and WD Harrison. Surficial glaciology of Jakobshavn's Isbræ, West Greenland: Part I. surface morphology. *Journal of Glaciology*, 37(127):368–382, 1991.

[20] I. Joughin, W. Abdalati, and M. Fahnestock. Large fluctuations in speed on Greenland's Jakobshavn Isbræ glacier. *Nature*, 432(7017):608–610, 2004.

[21] J.M. Amundson, M. Fahnestock, M. Truffer, J. Brown, M.P. Lüthi, and R.J. Motyka. Ice mélange dynamics and implications for terminus stability, Jakobshavn Isbræ, Greenland. *Journal of Geophysical Research*, 115(F1):F01005, 2010.

[22] I. Joughin, I.M. Howat, M. Fahnestock, B. Smith, W. Krabill, R.B. Alley, H. Stern, and M. Truffer. Continued evolution of Jakobshavn Isbræ following its rapid speedup. *Journal of Geophysical Research*, 113(F4):F04006, 2008.

[23] J.C. Plummer and C.J. van der Veen. A high-resolution bed elevation map for Jakobshavn Isbræ, West Greenland. In preparation, 2010.

[24] W.J.J. Van Pelt, J. Oerlemans, and C. H. Reijmer. Simulating melt, runoff and refreezing on Nordenskioldbreen using a coupled snow and energy balance model. *Journal of Glaciology*, 2011. In revision.

[25] H.J. Zwally, W. Abdalati, T. Herring, K. Larson, J. Saba, and K. Steffen. Surface melt-induced acceleration of Greenland ice-sheet flow. *Science*, 297(5579):218, 2002.

[26] I. Joughin, S.B. Das, M.A. King, B.E. Smith, I.M. Howat, and T. Moon. Seasonal speedup along the western flank of the Greenland ice sheet. *Science*, 320(5877):781, 2008.

[27] C. Schoof. A variational approach to ice stream flow. *Journal of Fluid Mechanics*, 556(1):227–251, 2006.

[28] D. R. MacAyeal. Large-scale ice flow over a viscous basal sediment: theory and application to ice stream B, Antarctica. *Journal of Geophysical Research*, 94(B4):4071–4087, 1989.

[29] G.K.C. Clarke. Subglacial processes. *Annual Review of Earth and Planetary Sciences*, 33:247–276, 2005.

[30] J.M. Amundson and M. Truffer. A unifying framework for iceberg-calving models. *Journal of Glaciology*, 56(199):822–830, 2010.

[31] R. Winkelmann, M. A. Martin, M. Haseloff, T. Albrecht, E. Bueler, C. Khroulev, and A. Levermann. The Potsdam Parallel Ice Sheet Model (PISM-PIK) Part 1: Model description. *The Cryosphere*, 5:715–726, 2011.

[32] T. Albrecht, M. Martin, M. Haseloff, R. Winkelmann, and A. Levermann. Parameterization for subgrid-scale motion of ice-shelf calving fronts. *The Cryosphere*, 5:35–44, 2011.

[33] D.M. Holland, R.H. Thomas, B. De Young, M.H. Ribergaard, and B. Lyberth. Acceleration of Jakobshavn Isbræ triggered by warm subsurface ocean waters. *Nature Geoscience*, 1(10):659–664, 2008.

[34] R.J. Motyka, M. Truffer, M. Fahnestock, J. Mortensen, S. Rysgaard, and I. Howat. Submarine melting of the 1985 Jakobshavn Isbræ floating tongue and the triggering of the current retreat. *Journal of Geophysical Research*, 116(F15):F01007, 2011.

[35] O.B. Christensen, M. Drews, J.H. Christensen, K. Dethloff, K. Ketelsen, I. Hebestadt, and A. Rinke. The HIRHAM regional climate model version 5 (β). *Danish Climate Center Report*, pages 06–17, 2008.

[36] N.M. Shapiro and M.H. Ritzwoller. Inferring surface heat flux distributions guided by a global seismic model: particular application to Antarctica. *Earth and Planetary Science Letters*, 223(1-2):213–224, 2004.

[37] R. A. Bindschadler, S. Nowicki, A. Aschwanden, E. Bueler, H. Choi, J. Fastook, R. Greve, and et al. SeaRISE: Sensitivities of Earth's Ice Sheets to their Environments. In preparation, 2012.

[38] M. Habermann, D. Maxwell, and M. Truffer. Stopping criteria for the reconstruction of basal properties in ice sheets. *Journal of Glaciology*, 2011. In revision.